Hindawi
Wireless Communications and Mobile Computing
Volume 2022, Article ID 6723403, 10 pages
https://doi.org/10.1155/2022/6723403

Research Article

UAV-Aided Multiuser Mobile Edge Computing Networks with Energy Harvesting

Changyu Wang,[1] Weili Yu,[1] Fusheng Zhu,[2] Jiangtao Ou,[3] Chengyuan Fan,[3] Jianghong Ou,[4] and Dahua Fan[4]

[1]*Aviation University Air Force, Changchun, Jilin, China*
[2]*Guangdong New Generation Communication and Network Innovative Institute (GDCNi), Guangzhou, China*
[3]*AI Sensing Technology, Foshan, Guangdong, China*
[4]*Starway Communication, Guangzhou, China*

Correspondence should be addressed to Fusheng Zhu; fushengzhu.gdcni@hotmail.com

Received 2 April 2022; Revised 16 April 2022; Accepted 21 April 2022; Published 21 June 2022

Academic Editor: Xingwang Li

This article studies a mobile edge computing (MEC) with one edge node (EN), where multiple unmanned aerial vehicles (UAVs) act as users which have some heavy tasks. As the users generally have limitations in both calculating and power supply, the EN can help calculate the tasks and meanwhile supply the power to the users through energy harvesting. We optimize the system by proposing a joint strategy to unpacking and energy harvesting. Specifically, a deep reinforcement learning (DRL) algorithm is implemented to provide a solution to the unpacking, while several analytical solutions are given to the power allocation of energy harvesting among multiple users. In particular, criterion I is the equivalent power allocation, criterion II is designed through equal data rate, while criterion III is based on the equivalent transmission delay. We finally give some results to verify the joint strategy for the UAV-aided multiuser MEC system with energy harvesting.

1. Introduction

In recent years, wireless communication has been put into many efforts from the researchers of both academy and industry [1, 2], which inspires a lot of practical applications, such as internet of things and video monitoring [3]. Among these applications, a key feature is that massive calculating is involved due to the massive number of accessing nodes [4]. To suppress the massive calculating, cloud computing has been proposed which assisted the task calculating through wireless transmission [5, 6]. A major limitation is that the latency and power consumption (PoC) become prohibitively high in a poor channel state, which limits the development and application of cloud computing severely.

To resolve the above disadvantages of cloud computing, mobile edge computing (MEC) has been proposed to install the calculating resources at the edge node (ENs) of the network [7–9]. In this way, the users can unpack the tasks to the nearby EN through wireless transmission, which leads to a decreased delay and PoC compared to the cloud computing. A key design in the MEC system is the unpacking scale [10, 11], which gives the number of scale of tasks to be calculated at the EN. The fundamental principle of unpacking is to jointly utilize the communication and calculating resources, through achieving a fine trade-off between the calculating and wireless transmission. Moreover, some advanced wireless techniques have been proposed to decrease the delay and PoC in the calculating and transmission [12, 13].

Another new technique to assist the calculating and communication in IoT networks is the deployment of unmanned aerial vehicles (UAVs), which are easy to be used and provide flexible ability. Moreover, the price of UAV is becoming cheaper and cheaper, which inspires a lot of applications in practice [14, 15]. For the MEC system, the UAVs can rescue the data calculating with higher priority through some intelligent path routing and scheduling, which exploits

the incremental system resources due to the usage of UAVs. The integration of UAVs into MEC systems has attracted much attention from the researchers of academy and industry, which becomes the motivation of this article.

Motivated by the above literature review, this article studies a MEC system with one EN, where multiple unmanned aerial vehicles (UAVs) act as users which have some heavy tasks. As the users generally have limitations in both calculating and power supply, the EN can help calculate the tasks and meanwhile supply the power to the users through energy harvesting. We optimize the system by proposing a joint strategy to unpacking and energy harvesting. Specifically, a deep reinforcement learning (DRL) algorithm is implemented to provide a solution to the unpacking, while several analytical solutions are given to the power allocation of energy harvesting among multiple users. In particular, criterion I is the equivalent power allocation, criterion II is designed through equal data rate, while criterion III is based on the equivalent transmission delay. We finally give some results to verify the joint strategy for the UAV-aided multiuser MEC system with energy harvesting.

2. System Model

In this paper, we consider an unloading system model in Figure 1 which has an edge node (EN) (note that the notation of "CAP" is used in some literature, while the notation "EN" is used in other literature. Both stand for the same meaning, and these two notations can be used interchangeably) surrounded by N unmanned aerial vehicles (UAVs). Specifically, the EN has an energy transmitter and a server which can provide calculating. The EN is capable of providing charging services to the UAVs, and each UAV is equipped with a limited battery capable of wireless charging. Each UAV has a calculating task l_n. Due to the UAVs' limited calculating power, each UAV unloads the calculating task to the EN in order to reduce the calculating time. The EN ensures that the UAV is always supplied with electricity, so the UAVs in this system unload tasks without considering power consumption. We will introduce the local calculating model and unloading calculating model in the next parts.

2.1. Local Calculating Model. The local calculating delay of the UAV_n is [16]

$$D^n_{\text{local}} = \frac{l_n(1-\beta^n_{\text{EN}})c}{f_n}, \tag{1}$$

where l_n is the size of the task. β^n_{EN} is the unloading ratio from UAV_n to the EN. Moreover, c is the CPU cycles for executing one bit, and f_n is the local calculating ability. Because all UAVs calculate their tasks in parallel, we use the maximum value of local calculating as the local delay of the whole system. So, the local calculating delay of the whole system is

$$D_{\text{local}} = \max\left\{D^1_{\text{local}}, D^2_{\text{local}}, \cdots, D^N_{\text{local}}\right\}. \tag{2}$$

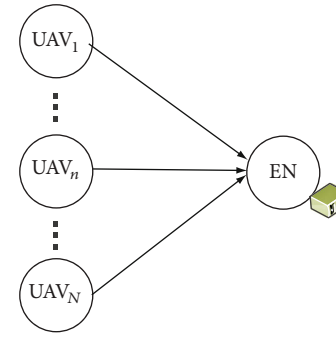

Figure 1: System model of multiuser MEC system with energy harvesting.

2.2. Unloading Calculating Model. In this paper, UAV_n will be charged by EN, and the charging process from EN to UAV_n is

$$H_n = \eta P^n_{\text{charge}} |h^n_{EN}|^2 \alpha_n \Gamma, \tag{3}$$

where notations η denotes the charging factor, P^n_{charge} is the charged power of EN, α_n is the charging time, and Γ denotes the span of each time slot.

From (3), the transmission power at the UAV_n is

$$P^n_{\text{tran}} = \frac{H_n}{(1-\alpha_n)\Gamma}. \tag{4}$$

The transmission rate between the UAV_n and the EN is

$$r^n_{\text{tran}} = W_{\text{total}} \log_2\left(1 + \frac{P^n_{\text{tran}}|h^n_{\text{EN}}|^2}{\sigma^2_{\text{EN}}}\right), \tag{5}$$

where W_{total} is the total bandwidth of the system. $h^n_{EN} \sim \mathscr{C}\mathcal{N}(0, \delta_{\text{EN}})$ is the channel parameter from UAV_n to the EN. σ^2_{EN} is the variance of the additive white Gaussian noise at the EN. The transmission delay of the UAV_n is

$$D^n_{\text{tran}} = \frac{l_n \beta^n_{EN}}{r^n_{\text{tran}}}. \tag{6}$$

The calculating delay at the UAV_n is

$$D^n_{\text{com}} = \frac{l_n \beta^n_{\text{EN}} c}{f_{\text{EN}}}, \tag{7}$$

where f_{EN} is the calculating ability at the EN. Further, the transmission delay of all UAVs is

$$D_{\text{tran}} = \max\left\{D^1_{\text{tran}}, D^2_{tran}, \cdots, D^N_{\text{tran}}\right\}. \tag{8}$$

The calculating delay of all UAVs is

$$D_{\text{com}} = \max\left\{D^1_{\text{com}}, D^2_{\text{com}}, \cdots, D^N_{\text{com}}\right\}. \tag{9}$$

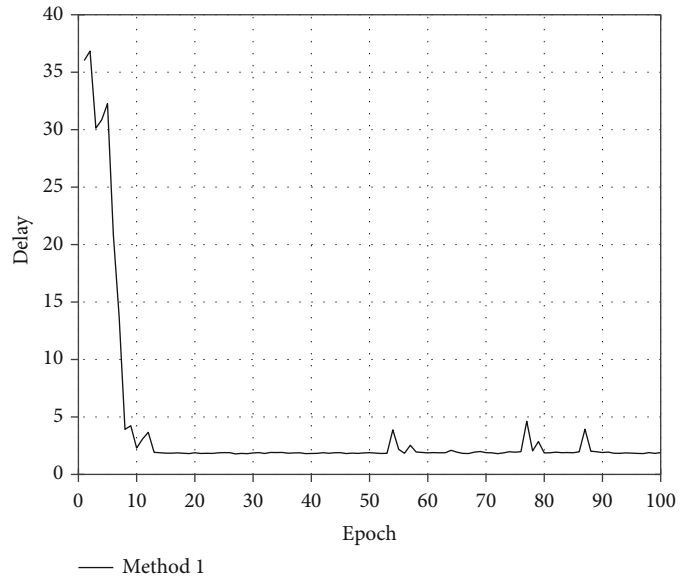

Figure 2: The convergence of method 1.

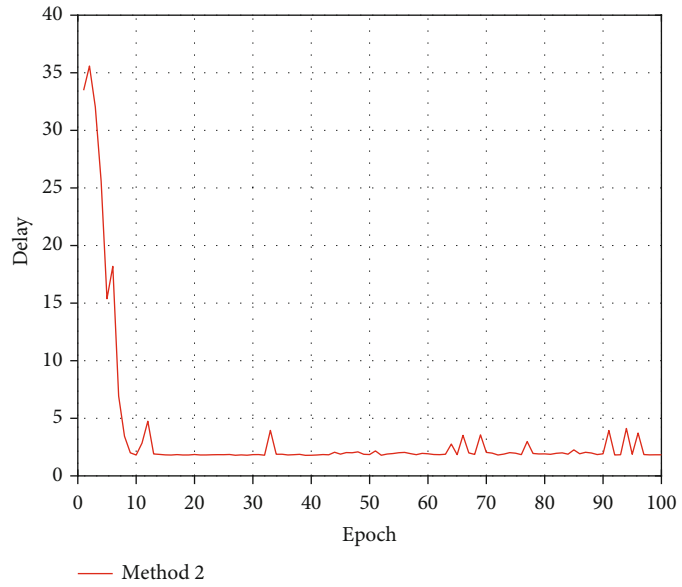

Figure 3: The convergence of method 2.

From (8) and (9), the unloading calculating of the whole system is

$$D_{\text{total}} = \max\{D_{\text{tran}}, D_{\text{com}}\}. \tag{10}$$

Therefore, the system target in this considered MEC network is

$$\begin{aligned} &\min_{\{\beta_n, P^n_{\text{charge}}\}} \Phi = D_{\text{total}} \\ &\text{s.t.} \quad C_1 : \beta^n_{\text{EN}} \in [0,1] \\ &C_2 : \sum_{n=1}^{N} P^n_{\text{charge}} = P^{\text{total}}_{\text{charge}}, \end{aligned} \tag{11}$$

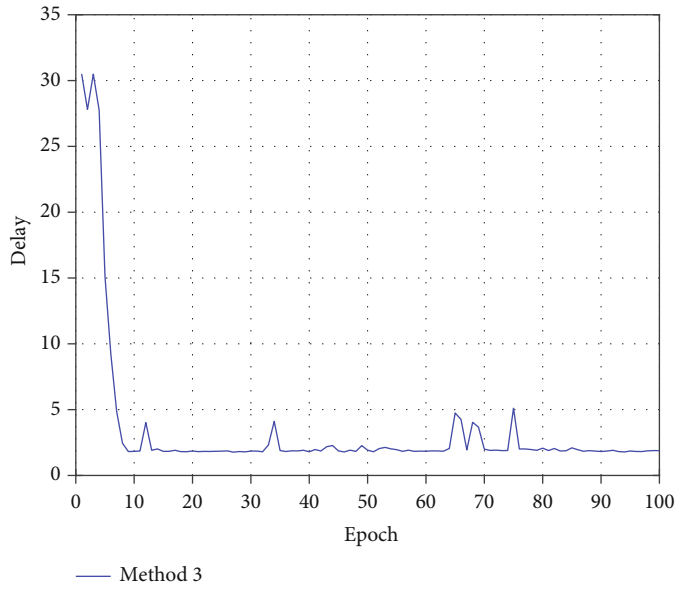

Figure 4: The convergence of method 3.

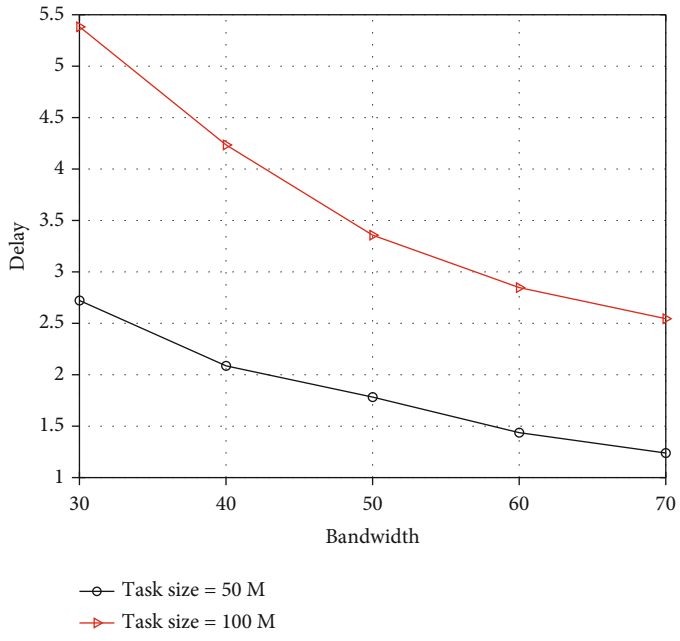

Figure 5: System delay of method 1 when the value of W_{total} ranges from 30 to 70.

where $P_{\text{charge}}^{\text{total}}$ is the total charged power of EN. In the next section, we will describe how we optimize the system target in detail.

3. System Optimization

In this section, we demonstrate our optimization scheme for the considered system target. Specifically, we first utilize deep Q-network (DQN) algorithm to obtain the task unloading strategy, and then, we proposed three methods to allocate the charged power for UAVs in the considered system. The details of our optimization scheme are expressed as follows.

3.1. Scheme on the Task Unloading. Due to the complexity of wireless link in the system, it is hard to dynamically unload the task of UAVs by traditional method. Therefore, we exploit DQN algorithm to obtain the task unloading strategy. Different from the Q-learning algorithm, DQN has an experience pool and two neural networks that include the evaluation network and the target network, to interact with the training environment and break the training data correlation.

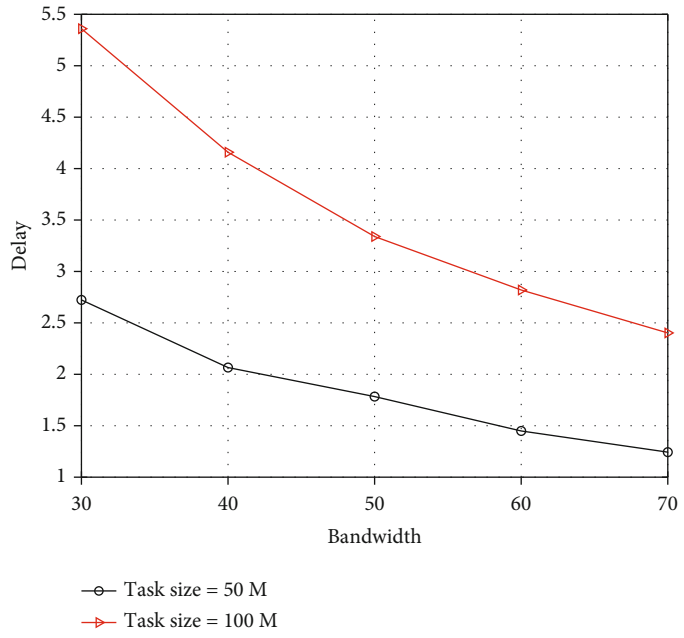

FIGURE 6: System delay of method 2 when the value of W_{total} ranges from 30 to 70.

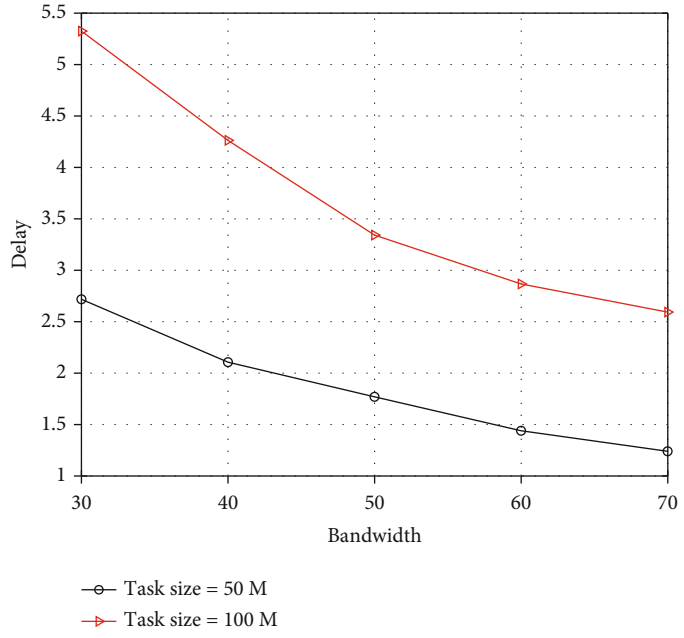

FIGURE 7: System delay of method 3 when the value of W_{total} ranges from 30 to 70.

Moreover, we use the Markov decision process (MDP) to model the consider task unloading issue. In particular, MDP generally consists of the state set $S = [s_1, s_2, \cdots, s_N]$, the action set $A = [a_1, a_2, \cdots, a_{2N}]$, and reward function $R = [0, -1, 1]$. The training process can be represented as follows: the DQN agent first initializes the system state set S, and then, it selects an action command under the current state. After the DQN agent executes the selected action command, the system state set will be updated. Further, the DQN agent will obtain a feedback according to the reward function R. Then, the DQN agent will put the previous state, the updated state, the selected action under the previous state, and the according feedback into the experience pool. When the DQN agent finishes the above process, it will obtain a state-action value $Q(S, A; \omega)$ that ω represents the network matrix of evaluation network. Then, the evaluation network will be trained by the loss function, which is

$$X = (Y - Q(S, A; \omega))^2, \tag{12}$$

where Y denotes the function of target network, which is

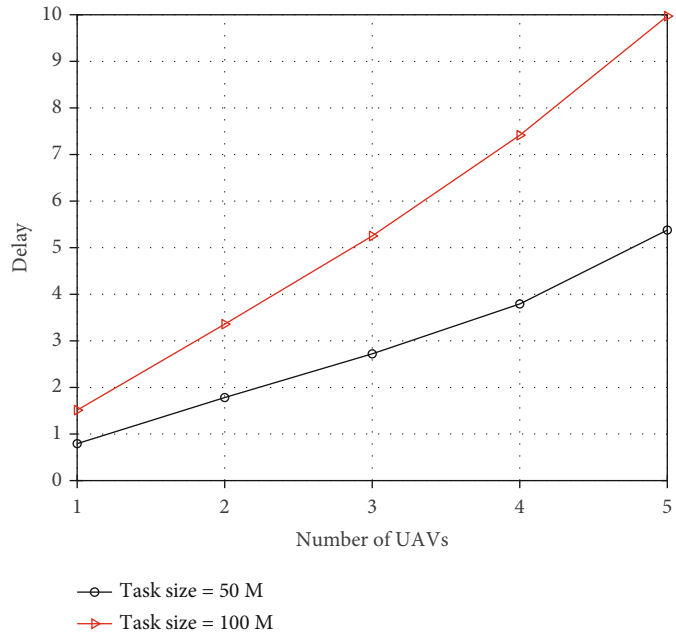

Figure 8: System delay versus the number of UAVs: method 1.

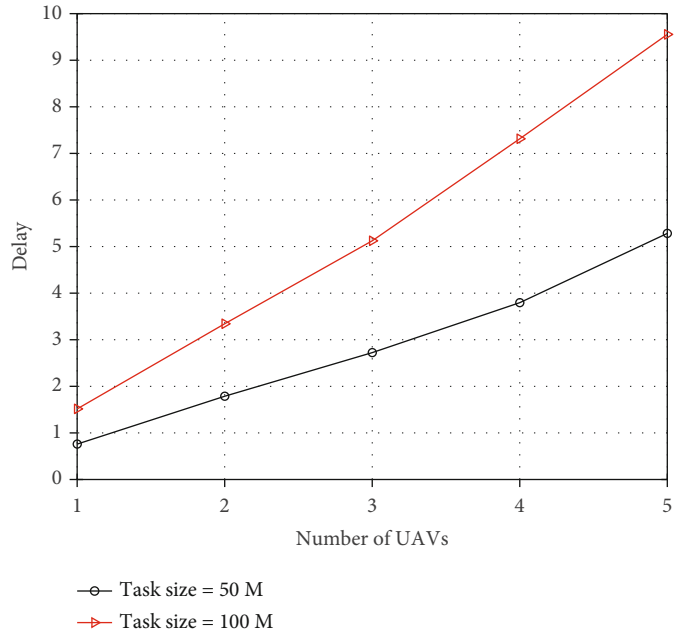

Figure 9: System delay versus the number of UAVs: method 2.

$$Y = R + \varphi \arg \max_{A^-} Q(S^-, A^-; \omega^*), \tag{13}$$

where φ represents a discount element and ω^* denotes the network matrix of the target network. It is notable that the structures of evaluation network and the target network are the same. However, different from the target network, the evaluation network will be trained in every round, and its training process can be denoted as

$$\omega^- = \omega - \xi \frac{\partial X}{\partial \omega}, \tag{14}$$

where ξ is the learning rate of the evaluation network.

3.2. Methods on the Charged Power Allocation. In this part, we will describe three methods for allocating the charged power from EN to UAV_n. Specifically, we exploit equal-

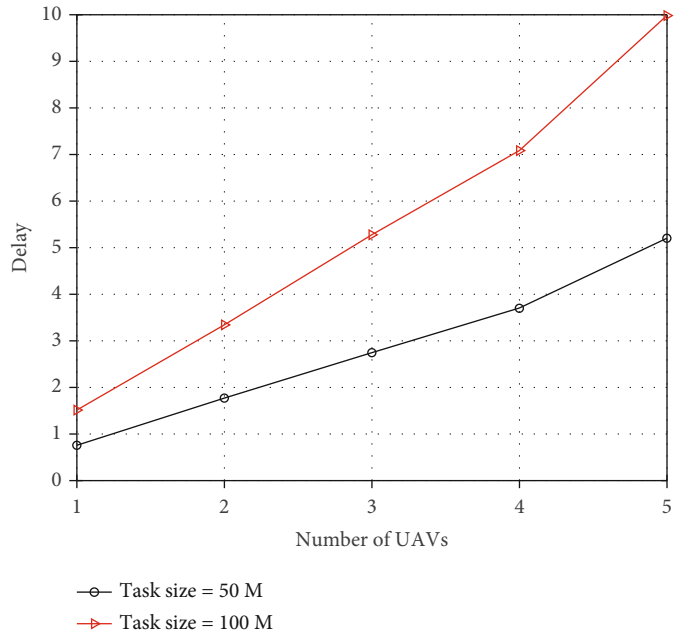

Figure 10: System delay versus the number of UAVs: method 3.

charge-power allocation method, equal-transmit-rate allocation method, and equal-charge-energy allocation.

(1) Equal-charge-power allocation method

Firstly, we allocate the charge power to UAV_n in a traditional way, so that each UAV_n can obtain the same charge power. Moreover, we define this method as equal-charge-power allocation method or method 1, and it can be denoted as

$$P_{\text{charge}}^{n} = \frac{P_{\text{charge}}^{\text{total}}}{N}, \tag{15}$$

where notation P_{charge}^{n} denotes the allocated charge power of UAV_n.

(2) Equal-transmission-rate allocation method

Secondly, we allocate the charge power to UAV_n by a method that ensure each UAV_n can obtain the same transmission rate according to (5). Moreover, we define this method as equal-transmission-rate allocation method or method 2. This method can be represented as

$$r_{\text{trans}}^{1} = r_{\text{trans}}^{2} = \cdots = r_{\text{trans}}^{N}. \tag{16}$$

From (16) and (5), we can obtain

$$W_{\text{total}} \log_2\left(1 + \frac{P_{\text{tran}}^{1}\left|h_{\text{EN}}^{1}\right|^2}{\sigma_{\text{EN}}^2}\right) = W_{\text{total}} \log_2\left(1 + \frac{P_{\text{tran}}^{2}\left|h_{\text{EN}}^{2}\right|^2}{\sigma_{EN}^2}\right) = \cdots = W_{\text{total}} \log_2\left(1 + \frac{P_{\text{tran}}^{N}\left|h_{\text{EN}}^{N}\right|^2}{\sigma_{\text{EN}}^2}\right). \tag{17}$$

By removing the common item of W_{total}, we can have

$$\log_2\left(1 + \frac{P_{\text{tran}}^{1}\left|h_{\text{EN}}^{1}\right|^2}{\sigma_{\text{EN}}^2}\right) = \log_2\left(1 + \frac{P_{\text{tran}}^{2}\left|h_{\text{EN}}^{2}\right|^2}{\sigma_{\text{EN}}^2}\right) = \cdots = \log_2\left(1 + \frac{P_{\text{tran}}^{N}\left|h_{\text{EN}}^{N}\right|^2}{\sigma_{\text{EN}}^2}\right). \tag{18}$$

From (4), we can obtain

$$\log_2\left(1 + \frac{H_1/(1-\alpha_1)\Gamma\left|h_{\text{EN}}^{1}\right|^2}{\sigma_{\text{EN}}^2}\right) = \log_2\left(1 + \frac{H_2/(1-\alpha_2)\Gamma\left|h_{\text{EN}}^{2}\right|^2}{\sigma_{\text{EN}}^2}\right) = \cdots = \log_2\left(1 + \frac{H_N/(1-\alpha_N)\Gamma\left|h_{\text{EN}}^{N}\right|^2}{\sigma_{\text{EN}}^2}\right), \tag{19}$$

$$1 + \frac{H_1/(1-\alpha_1)\Gamma\left|h_{\text{EN}}^{1}\right|^2}{\sigma_{\text{EN}}^2} = 1 + \frac{H_2/(1-\alpha_2)\Gamma\left|h_{\text{EN}}^{2}\right|^2}{\sigma_{\text{EN}}^2} = \cdots = 1 + \frac{H_N/(1-\alpha_N)\Gamma\left|h_{\text{EN}}^{N}\right|^2}{\sigma_{\text{EN}}^2}, \tag{20}$$

$$\frac{H_1/(1-\alpha_1)\Gamma\left|h_{\text{EN}}^{1}\right|^2}{\sigma_{\text{EN}}^2} = \frac{H_2/(1-\alpha_2)\Gamma\left|h_{\text{EN}}^{2}\right|^2}{\sigma_{EN}^2} = \cdots = \frac{H_N/(1-\alpha_N)\Gamma\left|h_{\text{EN}}^{N}\right|^2}{\sigma_{\text{EN}}^2}, \tag{21}$$

$$\frac{H_1}{(1-\alpha_1)\Gamma}\left|h_{\mathrm{EN}}^1\right|^2=\frac{H_2}{(1-\alpha_2)\Gamma}\left|h_{EN}^2\right|^2=\cdots=\frac{H_N}{(1-\alpha_N)\Gamma}\left|h_{\mathrm{EN}}^N\right|^2. \tag{22}$$

Moreover, from (3) and (22), we can obtain

$$\begin{aligned}\frac{\eta P_{\mathrm{charge}}^1\left|h_{\mathrm{EN}}^1\right|^2\alpha_1\Gamma}{(1-\alpha_1)\Gamma}\left|h_{\mathrm{EN}}^1\right|^2&=\frac{\eta P_{\mathrm{charge}}^2\left|h_{\mathrm{EN}}^2\right|^2\alpha_2\Gamma}{(1-\alpha_2)\Gamma}\left|h_{\mathrm{EN}}^2\right|^2\\&=\cdots=\frac{\eta P_{\mathrm{charge}}^N\left|h_{\mathrm{EN}}^N\right|^2\alpha_N\Gamma}{(1-\alpha_N)\Gamma}\left|h_{\mathrm{EN}}^N\right|^2.\end{aligned} \tag{23}$$

After removing the comment term of Γ, we can have

$$\begin{aligned}\frac{\eta P_{\mathrm{charge}}^1\left|h_{\mathrm{EN}}^1\right|^2\alpha_1}{(1-\alpha_1)}\left|h_{\mathrm{EN}}^1\right|^2&=\frac{\eta P_{\mathrm{charge}}^2\left|h_{\mathrm{EN}}^2\right|^2\alpha_2}{(1-\alpha_2)}\left|h_{\mathrm{EN}}^2\right|^2\\&=\cdots=\frac{\eta P_{\mathrm{charge}}^N\left|h_{\mathrm{EN}}^N\right|^2\alpha_N}{(1-\alpha_N)}\left|h_{\mathrm{EN}}^N\right|^2.\end{aligned} \tag{24}$$

Then, by further removing the comment term of η, we can have

$$\begin{aligned}\frac{P_{\mathrm{charge}}^1\left|h_{\mathrm{EN}}^1\right|^2\alpha_1}{(1-\alpha_1)}\left|h_{\mathrm{EN}}^1\right|^2&=\frac{P_{\mathrm{charge}}^2\left|h_{\mathrm{EN}}^2\right|^2\alpha_2}{(1-\alpha_2)}\left|h_{\mathrm{EN}}^2\right|^2\\&=\cdots=\frac{P_{\mathrm{charge}}^N\left|h_{\mathrm{EN}}^N\right|^2\alpha_N}{(1-\alpha_N)}\left|h_{\mathrm{EN}}^N\right|^2,\end{aligned} \tag{25}$$

$$\frac{P_{\mathrm{charge}}^1\left|h_{\mathrm{EN}}^1\right|^2\alpha_1}{(1-\alpha_1)}=\frac{P_{\mathrm{charge}}^2\left|h_{\mathrm{EN}}^2\right|^2\alpha_2}{(1-\alpha_2)}=\cdots=\frac{P_{\mathrm{charge}}^N\left|h_{\mathrm{EN}}^N\right|^2\alpha_N}{(1-\alpha_N)}. \tag{26}$$

For simplicity, we assume the charging time of each UAV is the same, which can be written as

$$\begin{aligned}\alpha_1=\alpha_2=\cdots=\alpha_N,\\(1-\alpha_1)=(1-\alpha_2)=\cdots=(1-\alpha_N).\end{aligned} \tag{27}$$

Therefore, from (26), we can obtain

$$\frac{P_{\mathrm{charge}}^1\left|h_{\mathrm{EN}}^1\right|^2}{(1-\alpha_1)}=\frac{P_{\mathrm{charge}}^2\left|h_{\mathrm{EN}}^2\right|^2}{(1-\alpha_2)}=\cdots=\frac{P_{\mathrm{charge}}^N\left|h_{\mathrm{EN}}^N\right|^2}{(1-\alpha_N)}. \tag{28}$$

By removing the common item of $(1-\alpha_n)$ for $n\in[1,N]$, we can have

$$P_{\mathrm{charge}}^1\left|h_{EN}^1\right|^2=P_{\mathrm{charge}}^2\left|h_{\mathrm{EN}}^2\right|^2=\cdots=P_{\mathrm{charge}}^N\left|h_{\mathrm{EN}}^N\right|^2. \tag{29}$$

From this equation, we have

$$\begin{aligned}P_{\mathrm{charge}}^1:P_{\mathrm{charge}}^2:\cdots:P_{\mathrm{charge}}^N=\left|h_{\mathrm{EN}}^1\right|^2:\left|h_{\mathrm{EN}}^2\right|^2:\cdots\\:\left|h_{\mathrm{EN}}^N\right|^2.\end{aligned} \tag{30}$$

Then, we can further obtain

$$\frac{P_{\mathrm{charge}}^n}{P_{\mathrm{charge}}^1+P_{\mathrm{charge}}^2+\cdots+P_{\mathrm{charge}}^N}=\frac{\left|h_{\mathrm{EN}}^n\right|^2}{\left|h_{\mathrm{EN}}^1\right|^2+\left|h_{\mathrm{EN}}^2\right|^2+\cdots+\left|h_{\mathrm{EN}}^N\right|^2}. \tag{31}$$

By using the relationship of $P_{\mathrm{charge}}^1+P_{\mathrm{charge}}^2+\cdots+P_{\mathrm{charge}}^N=P_{\mathrm{charge}}^{\mathrm{total}}$, we can have

$$\frac{P_{\mathrm{charge}}^n}{P_{\mathrm{charge}}^{\mathrm{total}}}=\frac{\left|h_{EN}^n\right|^2}{\left|h_{\mathrm{EN}}^1\right|^2+\left|h_{\mathrm{EN}}^2\right|^2+\cdots+\left|h_{\mathrm{EN}}^N\right|^2}. \tag{32}$$

From this equation, we can have the power charge allocation result of method 2 as

$$P_{\mathrm{charge}}^n=\frac{\left|h_{\mathrm{EN}}^n\right|^2}{\left|h_{\mathrm{EN}}^1\right|^2+\left|h_{\mathrm{EN}}^2\right|^2+\cdots+\left|h_{\mathrm{EN}}^N\right|^2}P_{\mathrm{charge}}^{\mathrm{total}}. \tag{33}$$

(3) Equal-charge-energy allocation method

Thirdly, we allocate the charge power to UAV_n by a method that ensure each UAV_n can be charged same energy according to (3). Moreover, we define this method as equal-charge-energy allocation method or method 3, which can be represented as

$$H_1=H_2=\cdots=H_N. \tag{34}$$

From (3), we can obtain

$$\eta P_{\mathrm{charge}}^1\left|h_{\mathrm{EN}}^1\right|^2\alpha_1\Gamma=\eta P_{\mathrm{charge}}^2\left|h_{\mathrm{EN}}^2\right|^2\alpha_2\Gamma=\cdots=\eta P_{\mathrm{charge}}^N\left|h_{\mathrm{EN}}^N\right|^2\alpha_N\Gamma. \tag{35}$$

By removing the common item of η, we can have

$$P_{\mathrm{charge}}^1\left|h_{\mathrm{EN}}^1\right|^2\alpha_1\Gamma=P_{\mathrm{charge}}^2\left|h_{\mathrm{EN}}^2\right|^2\alpha_2\Gamma=\cdots=P_{\mathrm{charge}}^N\left|h_{\mathrm{EN}}^N\right|^2\alpha_N\Gamma. \tag{36}$$

Then, by removing the common item of Γ, we can have

$$P_{\mathrm{charge}}^1\left|h_{\mathrm{EN}}^1\right|^2\alpha_1=P_{\mathrm{charge}}^2\left|h_{\mathrm{EN}}^2\right|^2\alpha_2=\cdots=P_{\mathrm{charge}}^N\left|h_{\mathrm{EN}}^N\right|^2\alpha_N. \tag{37}$$

Since we assume that the charging time of each UAV is

the same, we can further obtain

$$P^1_{\text{charge}}\left|h^1_{\text{EN}}\right|^2 = P^2_{\text{charge}}\left|h^2_{\text{EN}}\right|^2 = \cdots = P^N_{\text{charge}}\left|h^N_{\text{EN}}\right|^2,$$
$$P^1_{\text{charge}} : P^2_{\text{charge}} : \cdots : P^N_{\text{charge}} = \left|h^1_{\text{EN}}\right|^2 : \left|h^2_{\text{EN}}\right|^2 : \cdots : \left|h^N_{\text{EN}}\right|^2, \tag{38}$$

Then, we can further obtain

$$\frac{P^n_{\text{charge}}}{P^1_{\text{charge}} + P^2_{\text{charge}} + \cdots + P^N_{\text{charge}}} = \frac{\left|h^n_{\text{EN}}\right|^2}{\left|h^1_{\text{EN}}\right|^2 + \left|h^2_{\text{EN}}\right|^2 + \cdots + \left|h^N_{\text{EN}}\right|^2}. \tag{39}$$

By using the relationship of $P^1_{\text{charge}} + P^2_{\text{charge}} + \cdots + P^N_{\text{charge}} = P^{\text{total}}_{\text{charge}}$, we can have

$$\frac{P^n_{\text{charge}}}{P^{\text{total}}_{\text{charge}}} = \frac{\left|h^n_{\text{EN}}\right|^2}{\left|h^1_{\text{EN}}\right|^2 + \left|h^2_{\text{EN}}\right|^2 + \cdots + \left|h^N_{\text{EN}}\right|^2}. \tag{40}$$

From this equation, we can have the power charge result of method 3 as

$$P^n_{\text{charge}} = \frac{\left|h^n_{\text{EN}}\right|^2}{\left|h^1_{\text{EN}}\right|^2 + \left|h^2_{\text{EN}}\right|^2 + \cdots + \left|h^N_{EN}\right|^2} P^{\text{total}}_{\text{charge}}. \tag{41}$$

In the next section, we will perform some simulations to demonstrate the effectiveness of our proposed scheme on task offloading and charged power allocation.

4. Simulation

In this section, we perform some simulations to demonstrate our proposed scheme on task offloading and charged power allocation. Specifically, the channel in the considered MEC network adopts the Gaussian channel, and the average channel gain of the wireless link from UAVs to EN is set to 1. The variance of AWGN at the EN is set 0.1. Moreover, the number of UAVs is set to 2, and the task size of UAVs is set to 50 MB. We set the calculating ability of UAVs to 1.3×10^2 cycle/s, while the calculating ability of EN is set to 1×10^7 cycle/s. The total wireless bandwidth of EN is set to 50 MHz, and the total charged power of EN is set to 20 W, while the charging time of UAV is set 0.5.

Figure 2 shows the convergence of the proposed strategy with method 1. We can find that the system delay declines rapidly and converges after 15 epochs. For example, the system delay of method 1 decreases from 35 to less than 5. Similarly, Figures 3 and 4 show the convergence of the proposed strategy with methods 2 and 3, respectively. We can find that the system delay converges after 15 epochs and the value of delay eventually stabilised below five. These results demonstrate that the proposed DRL optimization strategy can effectively reduce the system delay and find the minimum value of the system delay.

Figure 5 shows the performance of the proposed strategy with method 1, where the value of W_{total} ranges from 30 to 70. When the task size of each UAV is 100M or 50M, the system delay decreases as W_{total} increases. This is because the increase in total bandwidth speeds up the transmission from the UAV to the EN and reduces system delay effectively. For example, the system delay at $W_{\text{total}} = 70$ is lower than the delay at $W_{\text{total}} = 30$. Similarly, Figures 6 and 7 show the performance of the proposed strategy with methods 2 and 3 when W_{total} ranges from 30 to 70, respectively. We can find that system delay decreases when the total bandwidth is increasing. These results demonstrate the effectiveness of proposed optimization strategy.

Figure 8 shows the performance of the proposed strategy with method 1, where the number of UAV ranges from 1 to 5. When the task size of each UAV is 100M or 50M, system delay increases as the number of UAVs increases. This i because the increase in the number of UAVs increases system burden and calculating delay. For example, the system delay when $n = 2$ is lower than the delay when $n = 5$. Similarly, Figures 9 and 10 show the performance of the proposed strategy with methods 2 and 3 when the number of UAVs ranges from 1 to 5, respectively. We can find that system delay increases when the number of UAVs is increasing. These results demonstrate that the proposed strategy can find the lowest system delay when the number of UAV ranges from 1 to 5.

5. Conclusions

This article studied a MEC system with one EN, where multiple unmanned aerial vehicles (UAVs) acted as users which had some heavy tasks. As the users generally had limitations in both calculating and power supply, the EN could help calculate the tasks and meanwhile supply the power to the users through energy harvesting. We optimized the system by proposing a joint strategy to unpacking and energy harvesting. Specifically, a deep reinforcement learning algorithm was implemented to provide a solution to the unpacking, while several analytical solutions were given to the power allocation of energy harvesting among multiple users. In particular, criterion I was the equivalent power allocation, criterion II was designed through equal data rate, while criterion III was based on the equivalent transmission delay. We finally gave some results to verify the joint strategy for the UAV-aided multiuser MEC system with energy harvesting.

Data Availability

The data can be obtained through email to the authors.

Conflicts of Interest

The authors declare that they have no conflicts of interest.

Acknowledgments

This work was supported by the Key-Area Research and Development Program of Guangdong Province (No. 2018B010124001).

References

[1] J. Xia, F. Zhou, X. Lai et al., "Cache aided decode-and-forward relaying networks: from the spatial view," *Wireless Communications and Mobile Computing*, vol. 2018, 9 pages, 2018.

[2] B. Wang, F. Gao, S. Jin, H. Lin, and G. Y. Li, "Spatial- and frequency-wideband effects in millimeter-wave massive MIMO systems," *IEEE Transactions on Signal Processing*, vol. 66, no. 13, pp. 3393–3406, 2018.

[3] X. Hu, C. Zhong, Y. Zhang, X. Chen, and Z. Zhang, "Location information aided multiple intelligent reflecting surface systems," *IEEE Transactions on Communications*, vol. 68, no. 12, pp. 7948–7962, 2020.

[4] H. Yan, L. Hu, X. Xiang, Z. Liu, and X. Yuan, "PPCL: Privacy-preserving collaborative learning for mitigating indirect information leakage," *Information Sciences*, vol. 548, pp. 423–437, 2021.

[5] Z. Su, F. Biennier, Z. Lv, Y. Peng, H. Song, and J. Miao, "Toward architectural and protocol-level foundation for end-to-end trustworthiness in cloud/fog computing," *IEEE Transactions on Big Data*, vol. 8, no. 1, pp. 35–47, 2022.

[6] M. T. Islam, S. Karunasekera, and R. Buyya, "Performance and cost-efficient spark job scheduling based on deep reinforcement learning in cloud computing environments," *IEEE Transactions on Parallel and Distributed Systems*, vol. 33, no. 7, pp. 1695–1710, 2022.

[7] X. Lai, L. Fan, X. Lei, Y. Deng, G. K. Karagiannidis, and A. Nallanathan, "Secure mobile edge computing networks in the presence of multiple eavesdroppers," *IEEE Transactions on Communications*, vol. 70, no. 1, pp. 500–513, 2022.

[8] J. Zhao, X. Sun, Q. Li, and X. Ma, "Edge caching and computation management for real-time internet of vehicles: an online and distributed approach," *IEEE Transactions on Intelligent Transportation Systems*, vol. 22, no. 4, pp. 2183–2197, 2021.

[9] L. Chen, R. Zhao, K. He, Z. Zhao, and L. Fan, "Intelligent ubiquitous computing for future UAV-enabled MEC network systems," *Cluster Computing*, vol. 2021, no. 1, pp. 1–11, 2021.

[10] F. Zhou and R. Q. Hu, "Computation efficiency maximization in wireless-powered mobile edge computing networks," *IEEE Transactions on Wireless Communications*, vol. 19, no. 5, pp. 3170–3184, 2020.

[11] F. Wang, H. Xing, and J. Xu, "Real-time resource allocation for wireless powered multiuser mobile edge computing with energy and task causality," *IEEE Transactions on Communications*, vol. 68, no. 11, pp. 7140–7155, 2020.

[12] W. Zhou, D. Deng, J. Xia, and Z. Shao, "The precoder design with covariance feedback for simultaneous information and energy transmission systems," *Wireless Communications and Mobile Computing*, vol. 2018, 17 pages, 2018.

[13] Q. Tao, J. Wang, and C. Zhong, "Performance analysis of intelligent reflecting surface aided communication systems," *IEEE Communications Letters*, vol. 24, no. 11, pp. 2464–2468, 2020.

[14] S. Arzykulov, A. Celik, G. Nauryzbayev, and A. M. Eltawil, "UAV-assisted cooperative & cognitive NOMA: deployment, clustering, and resource allocation," *IEEE Transactions on Cognitive Communications and Networking*, vol. 8, no. 1, pp. 263–281, 2022.

[15] R. Akbar, S. Prager, A. R. Silva, M. Moghaddam, and D. Entekhabi, "Wireless sensor network informed UAV path planning for soil moisture mapping," *IEEE Transactions on Geoscience and Remote Sensing*, vol. 60, pp. 1–13, 2022.

[16] J. Zhao, Q. Li, Y. Gong, and K. Zhang, "Computation offloading and resource allocation for cloud assisted mobile edge computing in vehicular networks," *IEEE Transactions on Vehicular Technology*, vol. 68, no. 8, pp. 7944–7956, 2019.